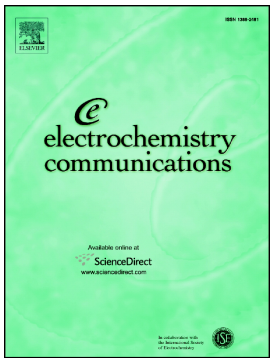

The kinetic origin of the Daumas-Hérold model for the Li-ion/ graphite intercalation system

E.M. Gavilán-Arriazu, O.A. Pinto, B.A. López de Mishima, D.E. Barraco, O.A. Oviedo, E.P.M. Leiva

PII: S1388-2481(18)30165-6
DOI: doi:10.1016/j.elecom.2018.07.004
Reference: ELECOM 6249

To appear in: *Electrochemistry Communications*

Received date: 31 May 2018
Revised date: 28 June 2018
Accepted date: 2 July 2018

Please cite this article as: E.M. Gavilán-Arriazu, O.A. Pinto, B.A. López de Mishima, D.E. Barraco, O.A. Oviedo, E.P.M. Leiva , The kinetic origin of the Daumas-Hérold model for the Li-ion/graphite intercalation system. Elecom (2018), doi:10.1016/ j.elecom.2018.07.004

The kinetic origin of the Daumas-Hérold model for the Li-ion /graphite intercalation system

[1,2]E. M. Gavilán-Arriazu, [2]O. A. Pinto, [2]B. A. López de Mishima, [3]D.E. Barraco, [1]O. A. Oviedo, [1]E. P. M. Leiva*

[1]Departamento de Química Teórica y Computacional, Facultad de Ciencias Químicas, Universidad Nacional de Córdoba, INFIQC, Córdoba, Argentina.

[2]Instituto de Bionanotecnología del NOA, Universidad Nacional de Santiago del Estero, Santiago del Estero, Argentina.

[3]Facultad de Matemática, Astronomía y Física, IFEG-CONICET, Universidad Nacional de Córdoba, Córdoba, Argentina.

*Corresponding author

maxigavilan@hotmail.com, eze_leiva@yahoo.com.ar

Abstract: Kinetic Monte Carlo simulations are applied to simulate the insertion of lithium ions into graphite. The present results show how the kinetics of lithium ion intercalation in graphite rules the global process, leading to metastable phases. The relatively slow rate of the events of insertion (deinsertion) of lithium ions into (from) graphite is found to yield the intercalation structures proposed by Daumas and Hérold. These arrangements can be be considered as frustrated, metastable structures, with a higher energy than that of the equilibrium state.

Keywords: lithium ion battery, kinetic Monte Carlo, Daumas-Hérold model, intercalation, graphite

1. Introduction

The understanding of the processes that occur in a graphite anode upon lithium ion insertion/deinsertion is a key factor to improve the performance of lithium-ion batteries.

Although numerous studies have been performed, the mechanisms that govern the kinetics of the intercalation process are still not well understood.

The Daumas-Hérold (DH) model [1] for Graphite intercalation compounds was proposed a long time ago and has been widely invoked in the literature to explain different features of intercalation phenomena. It assumes that intercalated ions occupy all graphite layers as a periodic arrangement of islands (clusters), as illustrated in Figure 1a. This model is often contrasted with the so-called Rüdorff-Hoffmann (RH) model [2], where for a given stage the occupation of the different layers shows no mismatches. In the original work of DH, the authors suggested that a possible reason for such an arrangement in potassium-graphite intercalation compounds was the presence of carbon monoxide, which occluded the possibility of potassium to migrate out of graphite, to be then reinserted into other graphite empty layers. This limitation would prevent the formation of the ordered structures predicted by the classic model. In the DH model, the formation of different stages would take place via rearrangements of the intercalant inside the lattice, without the need of whole layers being emptied/refilled to yield the different structures upon lithium loading/discharging. The question arises, however, what plays the role of carbon monoxide in limiting the entrance/exit of lithium inside/outside the graphite layers.

Numerous articles have been written on lithium intercalation in graphite, using a diversity of techniques. We point out some representative cases that applied the DH model for understanding experimental features found in lithium-graphite systems. Levi et al. [3, 4] performed fundamental electrochemical studies regarding Li-graphite systems and explained differences between experimental and simulated voltammetric current peaks in terms of lithium DH islands. Maurin et al. [5] found inhomogeneous swelling of multiwall carbon nanotubes upon lithium electrochemical intercalation, which was analyzed in terms of the DH model. Yamaki et al. [6] have observed two-phase separations like in DH model trough entropy calculations. Heβ and Novák [7] studied the Li ion-graphite kinetics with thin-layer electrodes, finding lithium (DH) domains. Sole et al. [8] got insight into Li intercalation in graphite performing in-Situ Raman espectroelectrochemical analysis. The behavior of the double resonance 2D band led these authors to support the DH model. Sethuraman et al. [9] obtained average Raman spectra of graphitic anodes cycling the electrodes in different potential windows. The origin of the surface structural disordering in graphite anodes upon different cycling conditions was revealed, considering the surface concentration gradient of Li in a DH scheme. Guo et al. [10] argued that Li injection kinetics influences the overall dynamics

of the system, making lithium to separate into “poor” and “rich” regions, as proposed by the DH model. A recent work from Allart et al. [11] proposes a new model to understand the lithium intercalation mechanism, assuming the existence of a new intermediate stage based on the DH model. Dimiev et al. [12] researched stage transitions trough optical microscopy and Raman spectroscopy, demonstrating the plausibility of the DH structural model. Some theoretical approaches from the 80’s focused on the kinetics of the DH model[13–15]. More recently, Krishnan et al. [16] have simulated the dynamics of lithium in graphite, giving a first clue around the importance of kinetics regarding the DH model.

Kinetic Monte Carlo (kMC) and Grand Canonical Monte Carlo (GCMC) methodologies are used here to tackle the present problem. GCMC simulations have been recently applied to lithium-ion studies in the literature [17,18]. Thus, both the kinetics and the thermodynamics of the system are considered. kMC is based on the idea that, if a system remains in a given state for a relatively long time, the system "forgets" how it arrived at that state. It overlooks the vibrational atomic motion allowing the simulation of considerably long times [19,20]. This aspect is particularly relevant for the case of the ion-Li / graphite system, where the intercalation phenomenon is a very slow process. In fact, voltammetric measurements involve potential sweep rates of around 4 μV / sec [3], lasting a typical voltammetric cycle of the order of a day or more.

2. Theoretical model and kinetic Monte Carlo method

A lattice-gas model was designed to follow the dynamical evolution of the system, where the ions were allowed to perform two types of events. First, to represent the existence of a surface, the ions could intercalate or deintercalate only at one side of the lattice (see Figure 1b). This insertion/deinsertion process reminds the insertion/deinsertion move allowed in Grand Canonical Monte Carlo (GCMC) simulations in our previous simulation work [17], but in the latter case, particles could enter to (or escape from) any site. The restriction of the creation/destruction move to surface sites in kMC bears important consequences for the delay of the equilibration process.

Ions were allowed to perform first-neighbor diffusion steps within each layer. This motion was restricted to the length of the graphite slab L_y in the case of the Y axes and it was completely free along the X axis, where periodic boundary conditions were applied (Figure 1b). The system was periodic in the Z direction. No jumps were allowed across the basal plane of graphite (Z direction).

This is reasonable, since the activation energy for lithium diffusion across the basal graphite plane amounts several eVs [21].

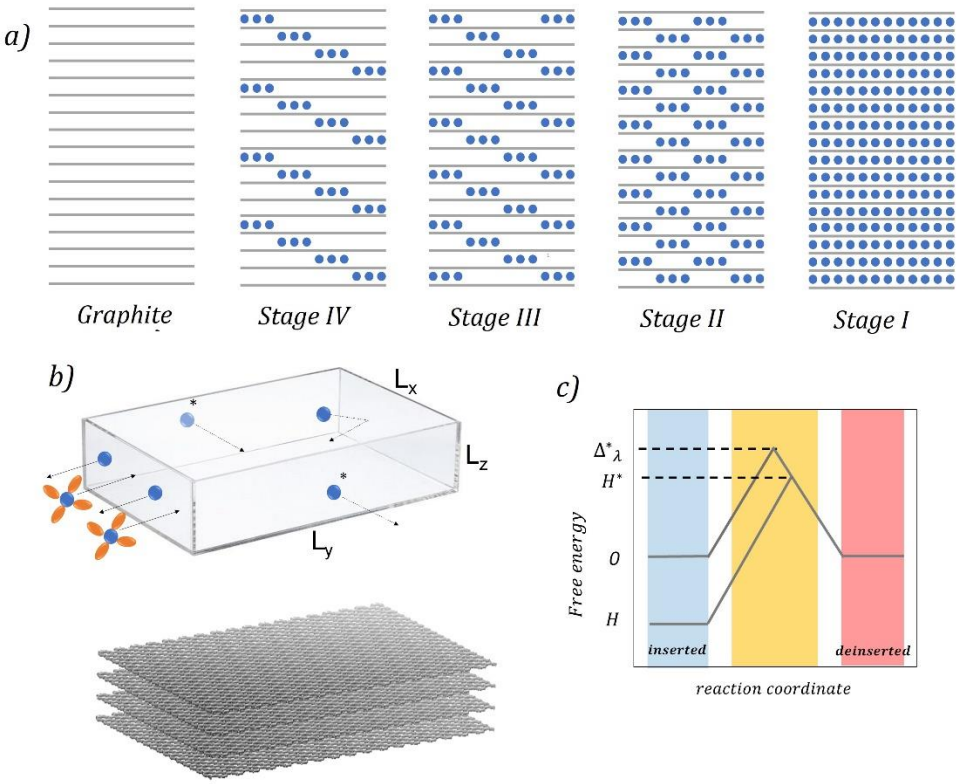

Figure 1: a) Dumas-Hérold model for lithium/graphite intercalation compounds. Lithium ions are represented in blue and graphite layers in grey. b) Simulation box. Ions are free to move in the X-Y plane, but not along the Z axis. The system is periodic in X and Z, but finite in the Y direction. The intercalation/deintercalation phenomenon occurs at one side of the lattice (interface). The atomic graphite arrangement is represented at the bottom of the figure and omitted in the upper part for simplicity. c) Scheme of the free energy barrier for the insertion/deinsertion process.

The Hamiltonian describing the system is the same as that used in References [17,22] to study the Li intercalation entropy and enthalpy and the critical temperature of the phase transition via MC simulations:

$$H = \sum_i^N \sum_{j\neq i}^{N_{ip}} \frac{c_i c_j \epsilon}{2}\left[\left(\frac{r_m}{r_{ij}}\right)^{12} - 2\left(\frac{r_m}{r_{ij}}\right)^{6}\right] + \sum_i^N \sum_j^{N_{op}} \frac{c_i c_j \kappa}{2}\left(\frac{r_b}{r_{ij}}\right)^{\alpha} + (\gamma - \mu)\sum_i^N c_i \qquad (1)$$

where N is the total number of lattice sites, N_{ip} is the number of neighbor sites in the same graphite plane and N_{op} is the number of neighbor sites in different graphite layers. Interactions are pairwise.

The first term is a Lennard-Jones potential and gives the attractive interaction between the Li-ions located in the same plane. c_i is an occupational term (1 occupied, 0 empty), r_{ij} is the distance between sites *i* and *j* belonging to the same plane and r_m is the second neighbor distance at which the potential reaches its minimum value ϵ. This term generates the $(\sqrt{3}x\sqrt{3})R30°$ ordered structure, characteristic of stage I and stage II. The second term was proposed by Derosa et al. [23] and describes the repulsion between Li-ions placed in different graphite layers. κ controls the repulsive interaction, r_{ij} is the distance between sites *i* and *j* from different planes, r_b is the C – C distance in graphite and α controls the interaction length. γ is the interaction energy between an inserted Li ion and the graphite substrate, and μ the chemical potential. For Lithium-graphite intercalation compounds, the open-circuit voltage (OCV) and μ are linearly related ($\mu=-e_0OCV$).

GCMC simulations were run comparatively; with insertion/deletion moves allowed at all lattice sites, using the geometry described in Figure 1b. No significant differences were found with respect to the results of Perassi et al. [17]. Elastic interactions were not taken into account, since electrostatic forces should prevail in intercalation compounds [16].

The rate constants for all processes were calculated following Ref [24,25]. The latter considers Butler-Volmer-type rates (2) to obtain the probability of the transition from an initial state *I* to a final state *F*. These are calculated according to (3):

$$\Gamma = v_0 \exp\left(-\frac{H^* - H_I}{k_B T}\right) \quad (2)$$

$$H^* = \Delta^*_\lambda + \alpha_{BV}(H_I + H_F) \quad (3)$$

where Γ is the reaction rate, v_0 is a preexponential factor associated with an effective vibrational frequency, k_B is the Boltzmann constant and *T* is the temperature. H_I, H_F and $H^*$are the energies of the initial, final and the transition state respectively. H_I and H_F are calculated from the Hamiltonian given in eq. (1), $\Delta^*_\lambda$is the energy barrier for the event λ when no interaction between the particles are considered (Figure 1c), i.e., when $H^* = \Delta^*_\lambda$. α_{BV} is the transfer coefficient.

Replacing eq. (3) in eq. (2) and taking $\alpha_{BV} = 1/2$:

$$\Gamma = v_0 \exp\left(-\frac{\Delta^*_\lambda}{k_B T}\right) \exp\left(-\frac{H_F - H_I}{2k_B T}\right) \quad (4)$$

which is the rate equation used.

The lattice-gas model used here consists in a four layers arrangement with triangular geometry of 18 x 36, the latter being the number of lateral sites at the X and Y axes. Each lattice site corresponds to the center of the C hexagon and the half distance between two graphite layers. For all rate constants (Eq. 4), the same pre-exponential factors $v_0 = 1x10^{13}\, s^{-1}$ was used [26,27]. The energy barriers for intercalation/deintercalation $\Delta^*_{i/di}$and diffusion Δ^*_d were fitted to yield experimental data of exchange current density [28] and diffusion coefficients in the low occupation limit [29].

3. Results and discussion

The temperature used was 296 K. It is remarkable that when we fitted $\Delta^*_{i/di}$ to yield the exchange current density measured by Chang et al., [28], the resulting energy barrier was $\Delta^*_{i/di} = 0.655\, eV$, which is very similar to the values found experimentally [30–32] and through very recent hybrid density functional and implicit solvation theory calculations [33]. A diffusional barrier $\Delta^*_d = 0.370\, eV$ was fitted using diffusion theory [34] and simulations within the canonical ensemble, to yield the value of the Li^+ diffusion coefficient at low occupations of the graphite lattice [29].

Figure 2a shows the occupation of the lattice for a kMC simulation of a potentiostatic step to $\mu = -0.095\, eV$ (electrode potential $0.095\, V$ vs Li/Li^+) starting from two different situations. First, from an empty lattice (black), which corresponds to a situation where $\mu \to -\infty$. Second, from a perfectly filled stage I (red), which corresponds to the limit $\mu \to +\infty$. The choice of the final chemical potential corresponds to a value where stage II is formed. In the first case, the Li-ion concentration is observed to increase with time, until oscillating around x ≈ 0.5. Steady state is reached at about 2 s. In the second case, the concentration decreases from x = 1.0 to x ≈ 0.5 and reaches a steady state at a similar time. Figure 2b shows a frame of a typical structure formed in both cases, yielding an energy per particle of -0.091 eV.

A GCMC simulation (equilibrium) was performed at the same chemical potential as before. After $1x10^7$ MC steps, a RH stage II is formed (Figure 2c). This structure results from the optimization of

attractive interactions within the same layer, and repulsive interaction between different layers. It is different from the kMC one reported above, yielding a lower energy per particle of -0.097 eV, that is, it is energetically more stable. It is clearly observed that while the GCMC result yields a "pure" or RH stage II structure, with a lower energy per particle, the kMC simulation delivers a typical DH structure, where a border between two mismatched stage II structures appears. To confirm the fact that the latter is a non-equilibrated structure, the following experiment was performed: after a long kMC simulation time, the kMC algorithm was "turned-off", and a GCMC was performed during $1x10^7$ MC steps. The result obtained was the expected one: when the GCMC algorithm was turned on, the system evolved from the "broken" stage II (Figure 2b) to the equilibrium-GCMC stage II (Figure 2c). These result show that the mismatched DH structure is the result of some kinetic hindrance of the system.

To understand the appearance of defective DH structures, we must think on the way in which the system evolves from an initial state to the steady state one. Let us analyze first the case of an initially empty lattice that becomes half-filled with Li ions when being subject to the proper chemical potential. At diluted concentrations (gas phase), Li ions occupy the network uniformly. Then, as the ion concentration increases, in-layer attractive interactions make Li ions to nucleate in ***all layers***. Since the energy barrier to escape from the system is relatively large, the exchange of ions with the environment through the electrode surface is too slow to allow equilibration towards a uniform stage II. Thus, a way to lower the energy with all layers occupied consist in building DH structures, which resemble Stage II, but with defects. So, if we assume that the approach to the more stable RH stage II is limited by ion exchange with the solution, increasing the adsorption/desorption rate (exchange current) should lead to this structure. To check this, the intercalation/deintercalation energy barrier was lowered ($\Delta^*_{i/di} = 0.380\ eV$), corresponding to an artificially large value of exchange current of (60 A / cm^2). The results for the energy of the system as a function of the simulated time are shown in Figure 2d. After $4.2x10^{-2}$ s (red line), the system goes naturally from the broken DH state (higher in energy) to the typical RH stage II structure obtained in the GCMC simulations.

4. Conclusions

The present work shows that the structures proposed in the Daumas-Hérold model are due to a kinetic limitation, which can be attributed to the slow process of insertion/deletion of lithium at the reaction surface. Ions initially present in all slabs, cannot get out and be reinserted again so as to accommodate in an alternate way, as required for a perfect stage II structure.

If equilibration of the system is forced by setting an artificially high exchange current density or by switching to a Grand Canonical Monte Carlo scheme, the structures turn to be those of the classical (Rüdorff-Hoffmann) model, where perfect stage II structures are formed. Thus, a way to suppress the occurrence of DH structures could be to increase the exchange current density in the experimental system, by changing for example the nature of the solvent. Alternatively, the use of ultra-small graphite flakes would favor ion exchange with the electrolyte, also suppressing the occurrence of DH structures.

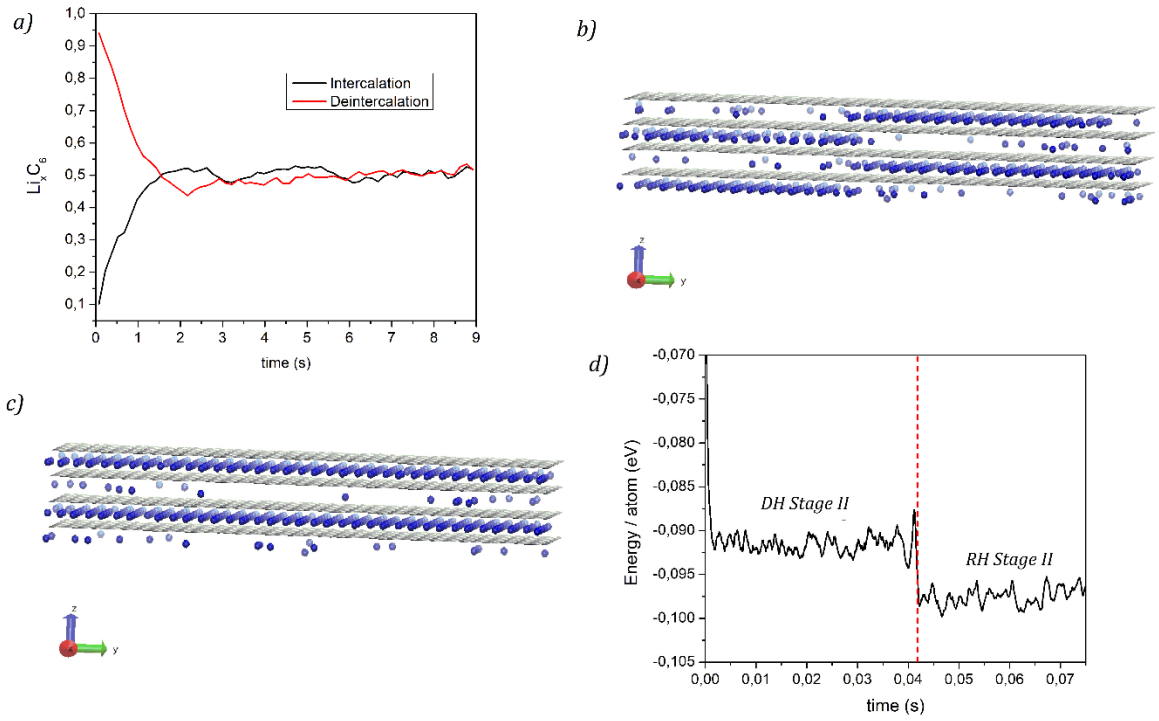

Figure 2: a) Time dependence of Li-ion deintercalation and intercalation. b) stage II formed with kMC simulations after 2 s. c) stage II formed with GCMC simulations. Li-ions are represented as blue spheres, graphite is the grey layer. d) Energy/atom vs time, obtained by reducing the insertion/deinsertion energy barrier

5. Acknowledgments

This work was supported by PIO Conicet-YPF 3855/15, PID Conicet-11220150100624, Program BID-Foncyt (PICT-2015-1605), SeCyT of the Universidad Nacional de Córdoba and YPF-Tecnología (Y-TEC), Argentina. Also, CONICET PIP 11220130100547CO and Universidad Nacional de Santiago del Estero under project CICyT-UNSE 23/A242, Argentina. An IPAC grant from SNCAD-MinCyT, Argentina is also acknowledged. A special thanks to Michael Mercer for helpful suggestions. E.M.G.A. acknowledges a CONICET fellowship.

6. References

[1] N. Daumas, A. Hérold, Notes des Membres et Correspon- tants et Notes Présentéesou Transmises par Leurs Soins, C. R. Acad. Sci. Ser. C. 268 (1969) 373–375.

[2] W. Rüdorff, U. Hofmann, Über Graphitsaelze, Zeitshrift Fur Anorg. Und Allg. Chemie. 238 (1938) 1–50. doi:10.1002/zaac.19382380102.

[3] M.D. Levi, D. Aurbach, The mechanism of lithium intercalation in graphite film electrodes in aprotic media. Part 1. High resolution slow scan rate cyclic voltammetric studies and modeling, J. Electroanal. Chem. 421 (1997) 79–88. doi:10.1016/S0022-0728(96)04832-2.

[4] M.D. Levi, E. a. Levi, D. Aurbach, The mechanism of lithium intercalation in graphite film electrodes in aprotic media. Part 2. Potentiostatic intermittent titration and in situ XRD studies of the solid-state ionic diffusion, J. Electroanal. Chem. 421 (1997) 89–97. doi:10.1016/S0022-0728(96)04833-4.

[5] G. Maurin, C. Bousquet, F. Henn, P. Bernier, R. Almairac, B. Simon, Electrochemical intercalation of lithium into multiwall carbon nanotubes, Chem. Phys. Lett. 312 (1999) 14–18. doi:10.1016/S0009-2614(99)00886-6.

[6] J. Yamaki, M. Egashira, S. Okada, Potential and Thermodynamics of Graphite Anodes in Li-Ion Cells, J. Electrochem. Soc. 147 (2000) 460. doi:10.1149/1.1393218.

[7] M. Heβ, P. Novák, Shrinking annuli mechanism and stage-dependent rate capability of thin-layer graphite electrodes for lithium-ion batteries, Electrochim. Acta. 106 (2013) 149–158. doi:10.1016/j.electacta.2013.05.056.

[8] C. Sole, N. Drewett, L. Hardwick, In situ Raman study of lithium-ion intercalation into microcrystalline graphite, Faraday Discuss. 172 (2014) 223–237. doi:10.1039/C4FD00079J.

[9] V.A. Sethuraman, L.J. Hardwick, V. Srinivasan, R. Kostecki, Surface structural disordering in graphite upon lithium intercalation/deintercalation, J. Power Sources. 195 (2010) 3655–3660. doi:10.1016/j.jpowsour.2009.12.034.

[10] Y. Guo, R.B. Smith, Z. Yu, D.K. Efetov, J. Wang, P. Kim, M.Z. Bazant, L.E. Brus, Li Intercalation into Graphite: Direct Optical Imaging and Cahn-Hilliard Reaction Dynamics, J. Phys. Chem. Lett. 7 (2016) 2151–2156. doi:10.1021/acs.jpclett.6b00625.

[11] D. Allart, M. Montaru, H. Gualous, Model of Lithium Intercalation into Graphite by Potentiometric Analysis with Equilibrium and Entropy Change Curves of Graphite Electrode, 165 (2018) 380–387. doi:10.1149/2.1251802jes.

[12] A.M. Dimiev, G. Ceriotti, N. Behabtu, D. Zakhidov, M. Pasquali, R. Saito, J.M. Tour, Direct real-time monitoring of stage transitions in graphite intercalation compounds, ACS Nano. 7 (2013) 2773–2780. doi:10.1021/nn400207e.

[13] S.A. Safran, D.R. Hamann, Long-Range Elastic Interactions and Staging in Graphite Intercalation Compounds, Phys. Rev. Lett. 42 (1979) 3–6. doi:10.1103/PhysRevLett.42.1410.

[14] S. Safran, D. Hamann, Electrostatic interactions and staging in graphite intercalation compounds, Phys. Rev. B. 22 (1980) 606–612. doi:10.1103/PhysRevB.22.606.

[15] G. Kirczenow, Kinetics of stage ordering and stage transitions, Phys. Rev. Lett. 55 (1985) 2810–2813. doi:10.1103/PhysRevLett.55.2810.

[16] S. Krishnan, G. Brenet, E. Machado-charry, D. Caliste, L. Genovese, T. Deutsch, P. Pochet, L. Genovese, T. Deutsch, P. Pochet, Revisiting the domain model for lithium intercalated graphite Revisiting the domain model for lithium intercalated graphite, Appl. Phys. Lett. 103 (2014) 251904. doi:10.1063/1.4850877.

[17] E.M. Perassi, E.P.M. Leiva, A theoretical model to determine intercalation entropy and enthalpy: Application to lithium/graphite, Electrochem. Commun. 65 (2016) 48–52. doi:10.1016/j.elecom.2016.02.003.

[18] M.P. Mercer, S. Finnigan, D. Kramer, D. Richards, H.E. Hoster, The influence of point defects on the entropy profiles of Lithium Ion Battery cathodes: a lattice-gas Monte Carlo study, Electrochim. Acta. 241 (2017) 141–152. doi:10.1016/j.electacta.2017.04.115.

[19] K.A. Fichthorn, W.H. Weinberg, Theoretical Foundations of Dynamical Monte Carlo Simulations, J. Chem. Phys. 95 (1991) 1090–1096. doi:10.1063/1.461138.

[20] A.F. Voter, INTRODUCTION TO THE KINETIC MONTE CARLO METHOD, in: K.E. Sickafus, E.A. Kotomin, B.P. Uberuaga (Eds.), Radiat. Eff. Solids, Springe, 2007: pp. 1–23. doi:10.1007/978-1-4020-5295-8_1.

[21] Y. Xin, A. Huang, Q. Hu, H. Shi, M. Wang, Z. Xiao, X. Zheng, Z. Di, P.K. Chu, Barrier Reduction of Lithium Ion Tunneling through Graphene with Hybrid Defects : First-Principles Calculations, Adv. Theory Simulations. 1 (2018) 1700009. doi:10.1002/adts.201700009.

[22] E.M. Gavilán Arriazu, B.A. López de Mishima, O.A. Oviedo, E.P.M. Leiva, O.A. Pinto, Criticality of the phase transition on stage two in a lattice-gas model of a graphite anode in a lithium-ion battery, Phys. Chem. Chem. Phys. 19 (2017) 23138–23145. doi:10.1039/C7CP04253A.

[23] P. a. Derosa, P.B. Balbuena, A Lattice-Gas Model Study of Lithium Intercalation in Graphite, J. Electrochem. Soc. 146 (1999) 3630. doi:10.1149/1.1392525.

[24] G. Brown, P.A. Rikvold, M.A. Novotny, A. Wieckowski, Simulated Dynamics of Underpotential Deposition of Cu with Sulfate on Au(111), J. Electrochem. Soc. 146 (1999) 1035–1040. doi:10.1149/1.1391717.

[25] S.J. Mitchell, G. Brown, P.A. Rikvold, Static and dynamic Monte Carlo simulations of Br

electrodeposition on Ag(1 0 0), Surf. Sci. 471 (2001) 125–142. doi:10.1016/S0039-6028(00)00892-X.

[26] K. Persson, Y. Hinuma, Y. Meng, A. Van der Ven, G. Ceder, Thermodynamic and kinetic properties of the Li-graphite system from first-principles calculations, Phys. Rev. B. 82 (2010) 1–9. doi:10.1103/PhysRevB.82.125416.

[27] K. Toyoura, Y. Koyama, A. Kuwabara, F. Oba, I. Tanaka, First-principles approach to chemical diffusion of lithium atoms in a graphite intercalation compound, Phys. Rev. B. 78 (2008) 1–12. doi:10.1103/PhysRevB.78.214303.

[28] Y. Chang, J. Jong, G.T. Fey, Kinetic Characterization of the Electrochemical Intercalation of Lithium Ions into Graphite Electrodes, J. Electrochem. Soc. 147 (2000) 2033–2038. doi:10.1149/1.1393481.

[29] M.D. Levi, D. Aurbach, Diffusion coefficients of lithium ions during intercalation into graphite derived from the simultaneous measurements and modeling of electrochemical impedance and potentiostatic intermittent titration characteristics of thin graphite electrodes, J. Phys. Chem. B. 101 (1997) 4641–4647. doi:10.1021/jp9701911.

[30] Y. Yamada, Y. Iriyama, T. Abe, Z. Ogumi, Kinetics of Lithium Ion Transfer at the Interface between Graphite and Liquid Electrolytes : Effects of Solvent and Surface Film, Langmuir. 25 (2009) 12766–12770. doi:10.1021/la901829v.

[31] K. Xu, A. Von Cresce, U. Lee, Differentiating Contributions to " Ion Transfer " Barrier from Interphasial Resistance and Li þ Desolvation at Electrolyte / Graphite Interface, Langmuir. 26 (2010) 11538–11543. doi:10.1021/la1009994.

[32] T. Abe, H. Fukuda, Y. Iriyama, Z. Ogumi, Solvated Li-Ion Transfer at Interface Between Graphite and Electrolyte, J. Electrochem. Soc. 151 (2004) 1120–1123. doi:10.1149/1.1763141.

[33] J. Haruyama, T. Ikeshoji, M. Otani, Analysis of Lithium Insertion / Desorption Reaction at Interfaces between Graphite Electrodes and Electrolyte Solution Using Density Functional + Implicit Solvation Theory, J. Phys. Chem. C. 122 (2018) 9804–9810. doi:10.1021/acs.jpcc.8b01979.

[34] D.A. Reed, G. Ehrlich, Surface diffusion, atomic jump rates and thermodynamics, Surf. Sci. 102 (1981) 588–609. doi:10.1016/0039-6028(81)90048-0.

Graphical abstract

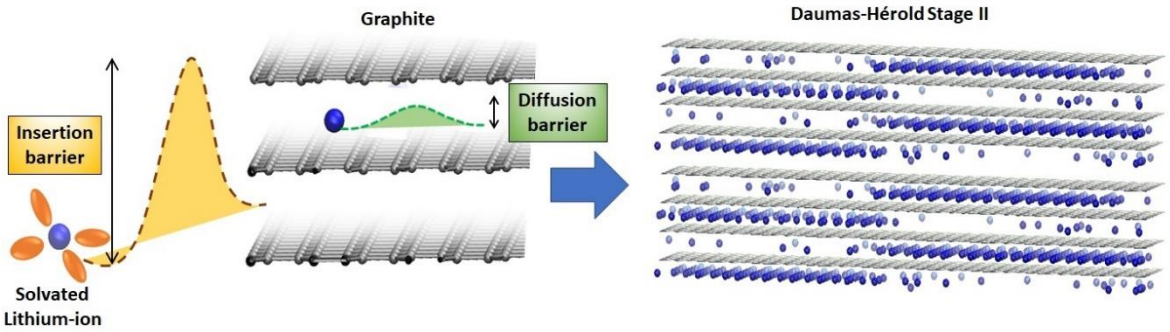

Highlights

- The kinetic origin of the Daumas-Hérold model for Lithium intercalation in graphite is elucidated
- Electrochemical intercalation is considered
- Grand Canonical Monte Carlo and kinetic Monte Carlo simulations are performed. comparatively
- The kinetics limitations arise due to a slow exchange on the lithium ions with the solution